Bioorganic & Medicinal Chemistry Letters 21 (2011) 3627–3631

Contents lists available at ScienceDirect

Bioorganic & Medicinal Chemistry Letters

journal homepage: www.elsevier.com/locate/bmcl

Discovery of a macrocyclic *o*-aminobenzamide Hsp90 inhibitor with heterocyclic tether that shows extended biomarker activity and in vivo efficacy in a mouse xenograft model

Christoph W. Zapf [a,*], Jonathan D. Bloom [a], Jamie L. McBean [a], Russell G. Dushin [a], Jennifer M. Golas [b], Hao Liu [b], Judy Lucas [b], Frank Boschelli [b], Erik Vogan [c], Jeremy I. Levin [a]

[a] Medicinal Chemistry, Pfizer, 401 N. Middletown Road, Pearl River, NY 10965, United States
[b] Oncology Research, Pfizer, 401 N. Middletown Road, Pearl River, NY 10965, United States
[c] Structural Biology & Computational Chemistry, Pfizer, 200 Cambridge Park Drive, Cambridge, MA 02139, United States

ARTICLE INFO

Article history:
Received 30 March 2011
Revised 18 April 2011
Accepted 21 April 2011
Available online 28 April 2011

Keywords:
Hsp90 inhibitors
Chaperone inhibitors
Ortho-aminobenzamides
N-terminal ATP-binding site
Macrocycles
Buchwald–Hartwig cyclization

ABSTRACT

A novel series of macrocyclic *ortho*-aminobenzamide Hsp90 inhibitors is reported. In continuation of our research, heterocycle-containing tethers were explored with the intent to further improve potency and minimize hERG liabilities. This effort culminated in the discovery of compound **10**, which efficiently suppressed proliferation of HCT116 and U87 cells. This compound showed prolonged Hsp90-inhibitory activity at least 24 h post-administration consistent with elevated and prolonged exposure in the tumor. When studied in a xenograft model, the compound demonstrated significant suppression of tumor growth.

© 2011 Elsevier Ltd. All rights reserved.

Modern cancer chemotherapy generally suffers from the emergence of drug resistance.[1,2] The selective silencing of a specific cell signaling pathway by a chemotherapeutic is arguably at the origin of this problem. By up-regulating alternative pathways, tumors are able to adapt to the drug treatment and continue their growth. Targeting chaperone proteins offers a promising solution to this traditional chemotherapy dilemma, since it allows the simultaneous inhibition of multiple pathways with a single agent.[3,4]

The ATP-dependent 90 kDa molecular chaperone Hsp90 has become an attractive target for cancer therapy.[5–10] It plays a critical role in maintaining the function of a wide range of client proteins, many of which are intimately involved in cancer pathology.[11] Inhibition of Hsp90 leads to the destabilization, and ultimately degradation of the clients, which results in the inhibition of cell growth and apoptosis.[12]

Different ATP-competitive chemotypes have evolved as potent *N*-terminal Hsp90 inhibitors, several of which have transitioned into clinical trials.[13–15] While many of these clinical trials focus on Hsp90 inhibitors as single agents for cancer therapy, combination studies with established chemotherapeutics have been designed and were reported recently as well.[16]

The first Hsp90 inhibitor reported in the literature was the macrocyclic natural product Geldanamycin **1** (Fig. 1), which belongs to the class of the ansamycins.[17] Clinical studies established this compound's unacceptable toxicology profile, preventing it from further development.[18] Optimization studies led to the discovery of 17-AAG **2** and 17-DMAG **3**[19] which are currently in clinical trials, but which are characterized by poor solubility and a narrow therapeutic window, respectively.

Vernalis recently disclosed resorcinol **4**[20] which entered clinical trials in 2007. Isoxazole **4** is one of many small molecules which have been described in the literature as potential novel Hsp90 inhibitors with clinical application and is part of a recent summary on this topic.[21]

Serenex recently disclosed their own efforts to discover potent small-molecule Hsp90 inhibitors that would be devoid of the drawbacks associated with Geldanamycin and its analogs.[22] Their studies culminated in a series of 2-aminobenzamides which exhibited low-nanomolar potencies in a proliferation assay. Among the reported compounds, glycine pro-drug SNX-5422 (**5**) was advanced to clinical trials.[23]

Using structure-based drug design, a series of potent benzisoxazoles as Hsp90 inhibitors was recently discovered.[24] Continuing the search for potent small molecule inhibitors of Hsp90, and guided by X-ray crystallography using a structural analog of **5**,

* Corresponding author. Tel.: +1 617 665 5602; fax: +1 617 665 5682.
E-mail address: christoph.zapf@pfizer.com (C.W. Zapf).

0960-894X/$ - see front matter © 2011 Elsevier Ltd. All rights reserved.
doi:10.1016/j.bmcl.2011.04.102

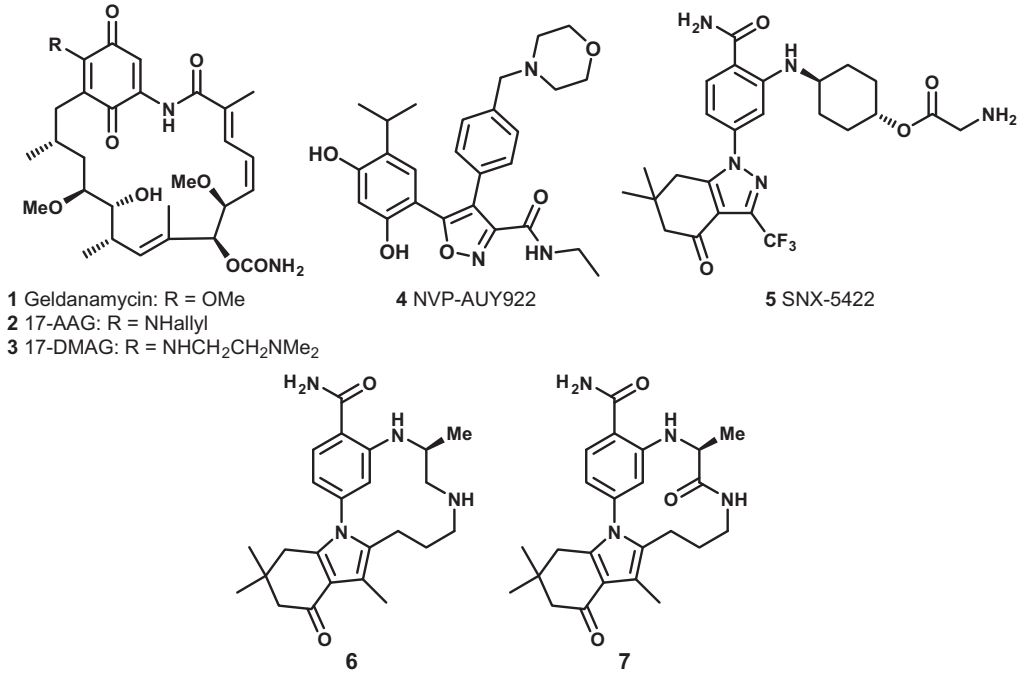

Figure 1. Structure of Geldanamycin **1**, clinically relevant ansamycins 17-AAG **2**, 17-DMAG **3**, Vernalis' clinical candidate NVP-AUY922 **4**, Serenex' clinical candidate SNX-5422 **5** as well as previously reported macrocyclic amine **6** and lactam **7**.

we were inspired to design structurally unique macrocycles[25,26] derived from *o*-aminobenzamides (such as amine **6**). These compounds were shown to be potent inhibitors of Hsp90 in an enzyme and cell-proliferation assay (HCT116) while retaining excellent solubility and microsomal stability.[27] Even more recently, we disclosed a series of macrocyclic amides (such as lactam **7**), which demonstrated excellent tumor exposure and biomarker activity even at 24 h post dosing while being devoid of activity at the hERG ionchannel.[28] We continued to seek compounds in this structure class that would demonstrate efficacy in a xenograft model and wish to disclose a design that involved the incorporation of small amine-based heterocyclic structures into the macrocyclic tether. This effort culminated in the discovery of macrocycle **10**, which showed in vivo efficacy in a glioma xenograft model.

As illustrated in Scheme 1, aldehyde **8**[27] was converted to amines **9** by reductive amination with either readily available or easily accessible optically pure building blocks, followed by removal of the Boc-protecting group. Cyclization using Buchwald–Hartwig conditions preceded hydrolysis of the aryl nitrile to the carboxamides **10**–**21**.

Analogs **22**–**27** (Fig. 2), with the exception of lactam **24**, were prepared using the same methodology as depicted in Scheme 1. Lactam **24** was prepared from the corresponding carboxylic acid utilizing identical chemistry as previously reported.[28]

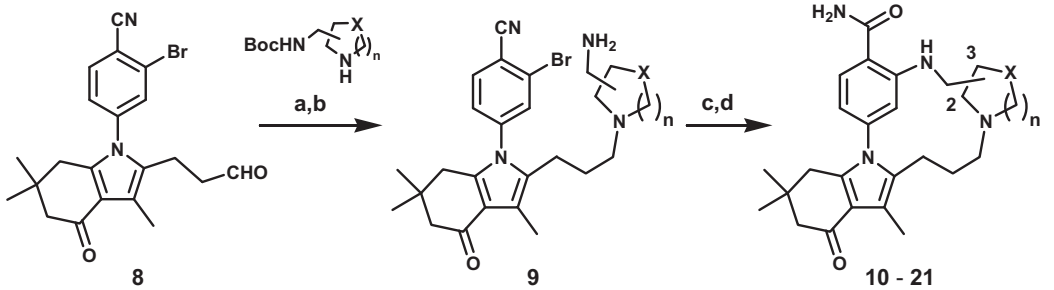

#	pos.	chirality	X	n
10	2	*R*	CH_2	1
11	2	*S*	CH_2	1
12	2	*R*	CH_2	2
13	2	*S*	O	2
14	2	S	NH	2
15	2	*S*	NAc	2

#	pos.	chirality	X	n
16	3	*R*	CH_2	1
17	3	*S*	CH_2	1
18	2	*R*	(R)-CHOH	1
19	2	*R*	(S)-CHF	1
20	2	*R*	(S)-CHNHAc	1
21	2	*R*	(*S*)-CH-N(CH_2)$_4$	1

Scheme 1. Reagents: (a) $NaBH(OAc)_3$, Boc-protected amine, DCE; (b) 10% TFA, DCM; (c) Pd_2dba_3, BINAP, NaO*t*Bu, dioxane, toluene, 110 °C; (d) 90% H_2SO_4, 60 °C or 5 M NaOH, 30% H_2O_2, DMSO, EtOH.

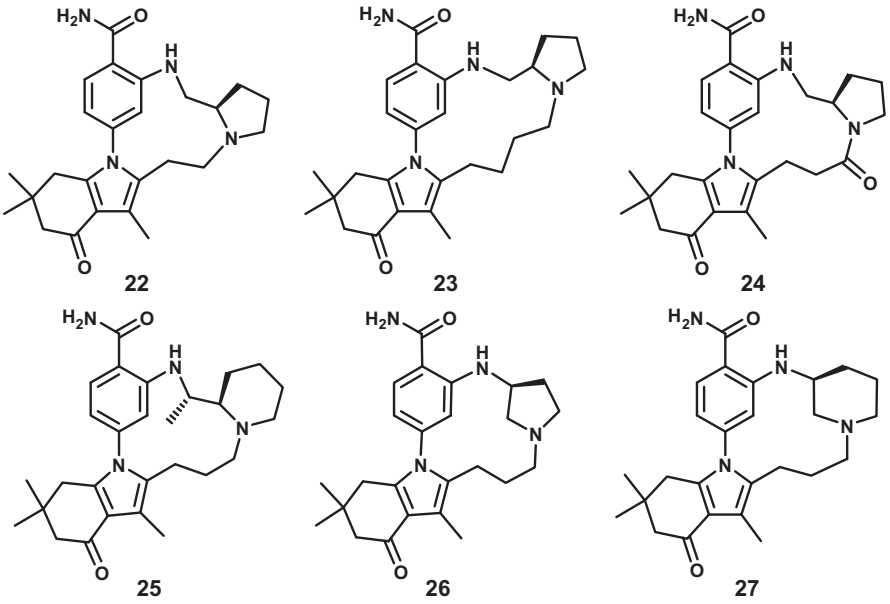

Figure 2. Analogs of macrocycle **10**, prepared in the attempt to improve stability and hERG activity.

One of the first macrocycles prepared in this series was pyrrolidine derivative **10**. It was designed as an analog to macrocycle **6** with the intent to improve its potency by incorporating a rigidifying structural element. Several heterocycle-containing 1,2-ethylenediamine derivatives are commercially available and were thus attractive building blocks for incorporation into the linker design. As expected, analog **10** showed an increase in potency compared to amine **6**, whereas its enantiomer **11** showed a substantial reduction in binding activity (Table 1). This finding underscores the critical nature of the stereochemical properties of the macrocyclic tether. Ring-size is another critical parameter that has a profound effect on potency. Compared to **10**, analogs **22** and **23** differ only by

Table 1
Biological activities, profiling data, and selected calculated properties for Geldanamycin and macrocycles **10**–**27**

#	Hsp90[a]	vSrc[b]	HCT116[c]	U87[c]	2C9[d]	2D6[d]	3A4[d]	Sol.[e]	Human[f]	Mouse[f]	Rat[f]	MW[g]	TPSA[h]	*c* log *P*[i]	hERG[j]	LE[k]	LipE[l]
1[m]	0.040	0.050	0.030	0.089	NT	NT	NT	NT	NT	NT	NT	561	163	2.1	NT	0.26	5.3
6	0.110	0.116	0.093	0.366	25	0	63	>100	10	NT	>30	409	89	4.1	NT	0.32	2.9
7	0.082	0.079	0.056	0.080	23	−5	6	>100	4	>30	>30	423	106	3.5	NT	0.32	3.6
10	0.096	0.040	0.032	0.087	6	34	73	2324	12	16	6	435	80	4.3	2.6	0.31	2.7
11	1.037	0.897	1.141	NT	NT	NT	NT	66	NT	NT	NT	435	80	4.3	NT	0.26	1.7
12	0.126	0.044	0.032	0.029	0	16	77	52	8	27	3	449	80	4.8	0.9	0.29	2.1
13	0.096	0.037	0.034	0.030	39	0	71	29	3	7	3	451	90	3.7	12.5	0.30	3.3
14	3.324	2.072	1.852	NT	−12	−3	1	>100	>30	>30	>30	450	92	3.7	NT	0.23	1.8
15	0.106	0.055	0.140	NT	15	4	34	>100	14	5	3	492	101	3.3	24.4	0.27	3.7
16	0.201	0.090	0.100	0.421	2	0	53	>100	23	>30	21	435	80	4.1	0.44	0.29	2.6
17	>5	3.607	2.973	NT	NT	NT	NT	NT	NT	NT	NT	435	80	4.1	NT	NT	NT
18	0.153	0.117	0.192	0.679	9	33	64	67	3	7	10	451	101	3.1	NT	0.29	3.7
19	0.061	0.036	0.060	0.095	46	9	77	3	4	5	2	453	80	4.3	16.4	0.31	2.9
20	0.634	1.491	2.564	3.628	NT	NT	NT	NT	NT	NT	NT	492	109	3.0	NT	0.24	3.2
21	0.496	1.836	2.428	>5	−3	69	34	71	NT	NT	5	504	84	4.4	NT	0.24	1.9
22	0.883	0.398	0.460	NT	0	6	32	6	NT	NT	6	421	80	3.9	NT	0.27	2.2
23	0.301	0.193	0.232	1.559	0	2	67	>100	5	11	8	449	80	4.8	NT	0.28	1.7
24	0.188	0.126	0.310	1.083	NT	NT	NT	NT	NT	NT	NT	449	97	3.2	NT	0.29	3.6
25	0.170	0.060	0.067	0.564	4	−4	55	35	3	6	7	463	80	5.4	1.5	0.28	1.4
26	0.982	0.582	0.671	NT	25	23	70	49	NT	NT	5	421	80	3.7	NT	0.27	2.3
27	0.078	0.081	0.039	0.067	74	12	76	16	2	3	8	435	80	4.3	3.4	0.31	2.8

For experimental details regarding assay conditions see Ref. 24.
[a] Enzyme IC_{50} (μM).
[b] Cell-based functional assay IC_{50} (μM).
[c] Cell-proliferation EC_{50} (μM).
[d] % Cyp-inhibition at 3 μM.
[e] Solubility (μg/mL).
[f] $t_{1/2}$ in microsomes (min).
[g] Molecular weight.
[h] Total polar surface area.
[i] Calculated partition ratio.
[j] Ion channel IC_{50} (μM).
[k] Ligand efficiency.
[l] Lipophilic efficiency.
[m] In-house data.

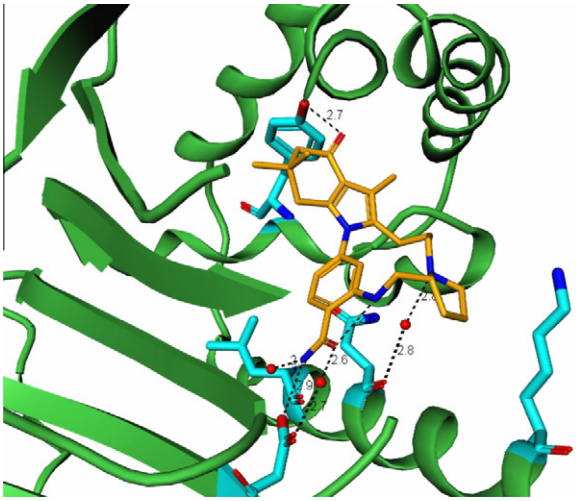

Figure 3. Macrocycle **10** bound to the *N*-terminal ATP-binding site of Hsp90. Hydrogen bonds (black dotted lines) are labeled with distances in Å. A portion of the peptide has been omitted for clarity.

one carbon atom, but exhibit a substantial reduction in activity. Likewise, removal of the basicity of the tether by conversion to an amide (**24**)—a strategy that had been productive previously[28]—leads to a significant loss in potency in this case.

Parallel to these efforts, the ring size and nature of the heterocyclic moiety within the tether was varied as well. Thus, stereochemically defined analogs **12**–**14** were prepared with a piperidine, morpholine and piperazine, in the linker, respectively (priority rules lead to a formal switch in stereochemical designation, Scheme 1). While **12** and **13** showed essentially identical activity compared to **10**, the drop in activity for **14** can be explained by the proximity of Lys58 (Fig. 3). Indeed, X-ray analysis of **14** reveals a water mediated interaction of the distal piperazine nitrogen with Lys58 (structure not shown). As expected, installation of the acetamide in analog **15** restores enzyme potency, providing a clear SAR trend for this series.

We had previously demonstrated that the potency of these macrocycles depends significantly on the overall conformational flexibility in the tether.[27,28] Extension of this concept to macrocycle **12** led to the design of analog **25** (Fig. 2), which was derived from an aminomethyl piperidine building block,[29] incorporating the stereochemically defined additional methyl group. Based on molecular modeling, analog **25** was the only diastereomer considered for this effort that did not yield the anticipated increase in activity. Based on this result, it was concluded that the heterocyclic tether itself appears to provide maximum productive rigidity compared to the acyclic tethers as in **6**.

An unexpected result was obtained when the connectivity of the pyrrolidine moiety in **10** was altered by moving the methylene group from position 2 to 3, de facto increasing the ring-size from 12 to 13. While again a clear stereochemical preference was observed for the two analogs **16** and **17**, the former was quite potent when considering that other 13-membered macrocycles had been substantially less active. By removing the methylene unit adjacent to the aniline nitrogen in **10** or **12** while maintaining connectivity to the 3-position of the heterocycle, 12-membered macrocycles **26** and **27** were obtained. In this instance, piperidine **27** was superior to pyrrolidine analog **26** and showed comparable potency to pyrrolidine **10**, without improving microsomal stability.

This latter group of analogs led to the conclusion that this connectivity pattern did not provide any of the required improvements. Thus, attention was directed toward the substitution of the pyrrolidine ring, with the goal of enhancing the properties associated with **10**. A high *c* log *P* was presumably predictive of its low stability in microsomes of the three indicated species (Table 1). Incorporation of a hydroxyl group (**18**) led to a reduction in lipophilicity but did not improve stability. Addition of a fluorine substituent (**19**) lowered the pK_a of the compound, which led to an improvement of the compound's potency at the hERG ion channel without affecting potency. However, no improvement of microsomal stability was observed, possibly due to the unchanged *c* log *P*. Addition of an acetamide (**20**) or pyrrolidine substituent (**21**) led to analogs with substantially reduced activity in the enzyme and cell-assays.

An X-ray crystal structure for macrocycle **10** bound to the *N*-terminal ATP-binding site of Hsp90 was obtained.[30] As can be seen in Figure 3, the carbonyl of the tetrahydroindolone engages in a hydrogen bond with Tyr139, while the benzamide interacts with Asp93 in a direct and a water-mediated hydrogen bond. The nitrogen of the tether forms an additional water-mediated interaction with the main chain carbonyl of Asn51. Figure 3 shows a second water molecule proximal to the benzamide interacting with Leu48 and Ser52, representing the dense network of conserved water molecules characteristic for the *N*-terminal ATP-binding site of Hsp90.

Figure 3 also highlights the proximity of Lys58 to the heterocyclic portion of the tether. This provides a structural explanation for the lack of potency of analogs bearing basic functionality approaching this side-chain.

The *o*-aminobenzamide-derived macrocyclic compounds bind to the *N*-terminal ATP binding pocket of ATP (Fig. 3) and are as such competitive ATP inhibitors. However, a substantial conformational difference can be noted when comparing the binding conformation of ATP in the active site of Hsp90 with its conformation in kinases. When **10** was submitted to the Invitrogen panel of 59 kinases, it was found that this compound displays only modest inhibitory activity for FYN (IC_{50} = 22 μM), a SRC-related membrane-associated tyrosine kinase, and inhibits the other kinases with an IC_{50} >50 μM.

Compound **10** was evaluated in a biomarker study in a xenograft model using U87 tumors (Fig. 4). When administered at 100 mg/kg iv, the compound clearly elicits a heat-shock response, characterized by an up-regulation of Hsp70, which is detectable even 24 h post dosing. Another characteristic response to effective Hsp90 inhibition, which was detected in the biomarker study, is

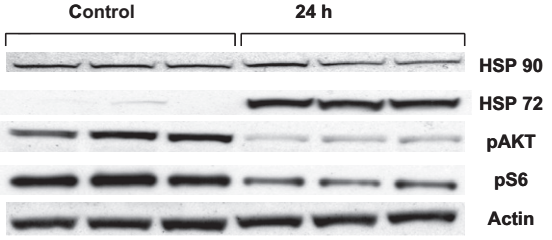

Figure 4. Biomarker results for compound **10** when dosed at 100 mg/kg iv in U87 bearing nude mice.

Table 2
Exposure levels of **10** in U87 xenograft tumors

Dose (mg/kg)	Route	Plasma (ng/mL) 24 h	Tumor (ng/g) 24 h
25	PO	18	109
50	PO	34	303
75	PO	67	476
100	PO	103	198
100	iv	90	1463

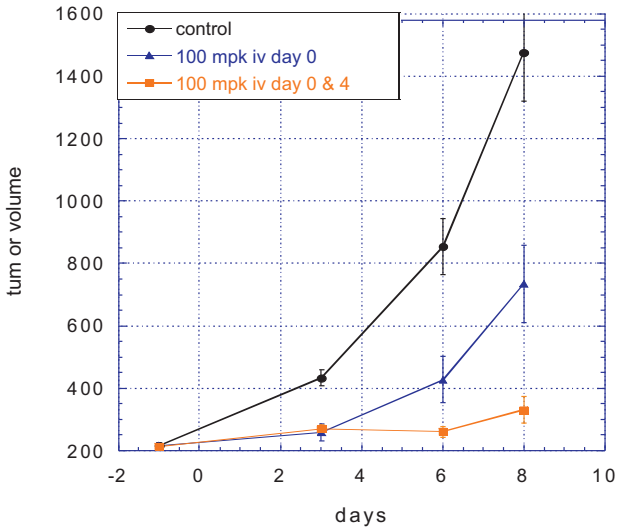

Figure 5. In vivo efficacy of analog **10** in U87 glioma bearing nude mice.

Table 3
PK parameters for **10** in male CD-1 mice following a single 2 mg/kg IV or 10 mg/kg oral dose

	$t_{1/2}$ (h)	AUC_{0-inf} (h ng/mL)	Clp (mL/min/kg)	V_{ss} (l/kg)	%F
iv	4.6	1738	19	5.3	74%
PO	5.2	6455			

the down-regulation of pS6 and pAKT, two known substrates for this chaperone.

Tissue and blood levels of **10** were also measured following iv and oral dosing. As can be seen in Table 2, clearance of the compound was observed from the blood 24 h post dosing. Compound levels in the tumor remained elevated throughout the 24 h experiment, generally in a dose-dependent manner consistent with the biomarker results. However, tumor exposure was substantially higher after iv compared to oral dosing.

Finally, compound **10** was characterized in a xenograft model using U87 bearing nude mice (Fig. 5). Compared to the control group, the macrocycle significantly suppressed tumor growth when dosed iv once at 100 mg/kg on day 0. The compound was even more effective when dosed twice per week at 100 mg/kg on days 0 and 4.

In conclusion, compound **10** was demonstrated to be a potent Hsp90 inhibitor in enzyme and cell-based assays. It showed excellent biomarker activity and a significant effect on tumor growth suppression. Furthermore, it demonstrated good tumor exposure 24 h after dosing and its pharmacokinetic parameters (Table 3) showed a good half-life ($t_{1/2}$) and exposure (AUC_{0-inf}), low plasma clearance (Clp), high volume of distribution at steady-state (V_{ss}) and high bioavailability (%F).

References and notes

1. Borst, P.; Jonkers, J.; Rottenberg, S. *Cell Cycle* **2007**, *6*, 2782.
2. Nobili, S.; Landini, I.; Giglioni, B.; Mini, E. *Curr. Drug Targets* **2006**, *7*, 861.
3. Blagg, B. S.; Kerr, T. D. *Med. Res. Rev.* **2006**, *26*, 310.
4. Neckers, L. *J. Biosci.* **2007**, *32*, 517.
5. Isaacs, J. S.; Xu, W.; Neckers, L. *Cancer Cell* **2003**, *3*, 213.
6. Solit, D. B.; Chiosis, G. *Drug Discovery Today* **2008**, *13*, 38.
7. Johnson, V. A.; Singh, E. K.; Nazarova, L. A.; Alexander, L. D.; McAlpine, S. R. *Curr. Top. Med. Chem.* **2010**, *10*, 1380.
8. Li, Y.; Zhang, T.; Schwartz, S. J.; Sun, D. *Drug Resist. Updates* **2009**, *12*, 17.
9. Janin, Y. L. *Drug Discovery Today* **2010**, *15*, 342.
10. Winssinger, N.; Fontaine, J. G.; Barluenga, S. *Curr. Top. Med. Chem.* **2009**, *9*, 1419.
11. Whitesell, L.; Lindquist, S. L. *Nat. Rev. Cancer* **2005**, *5*, 761.
12. Maloney, A.; Workman, P. *Expert Opin. Biol. Ther.* **2002**, *2*, 3.
13. Drysdale, M. J.; Brough, P. A. *Curr. Top. Med. Chem.* **2008**, *8*, 859.
14. Messaoudi, S.; Peyrat, J. F.; Brion, J. D.; Alami, M. *Anticancer Agents Med. Chem.* **2008**, *8*, 761.
15. Taldone, T.; Sun, W.; Chiosis, G. *Bioorg. Med. Chem.* **2009**, *17*, 2225.
16. Hwang, M.; Moretti, L.; Lu, B. *Curr. Med. Chem.* **2009**, *16*, 3081.
17. Whitesell, L.; Mimnaugh, E. G.; De Costa, B.; Myers, C. E.; Neckers, L. M. *Proc. Natl. Acad. Sci. U.S.A.* **1994**, *91*, 8324.
18. Supko, J. G.; Hickman, R. L.; Grever, M. R.; Malspeis, L. *Cancer Chemother. Pharmacol.* **1995**, *36*, 305.
19. Tian, Z. Q.; Liu, Y.; Zhang, D.; Wang, Z.; Dong, S. D.; Carreras, C. W.; Zhou, Y.; Rastelli, G.; Santi, D. V.; Myles, D. C. *Bioorg. Med. Chem.* **2004**, *12*, 5317.
20. Brough, P. A.; Aherne, W.; Barril, X.; Borgognoni, J.; Boxall, K.; Cansfield, J. E.; Cheung, K. M.; Collins, I.; Davies, N. G.; Drysdale, M. J.; Dymock, B.; Eccles, S. A.; Finch, H.; Fink, A.; Hayes, A.; Howes, R.; Hubbard, R. E.; James, K.; Jordan, A. M.; Lockie, A.; Martins, V.; Massey, A.; Matthews, T. P.; McDonald, E.; Northfield, C. J.; Pearl, L. H.; Prodromou, C.; Ray, S.; Raynaud, F. I.; Roughley, S. D.; Sharp, S. Y.; Surgenor, A.; Walmsley, D. L.; Webb, P.; Wood, M.; Workman, P.; Wright, L. *J. Med. Chem.* **2008**, *51*, 196.
21. Biamonte, M. A.; Van de Water, R.; Arndt, J. W.; Scannevin, R. H.; Perret, D.; Lee, W. C. *J. Med. Chem.* **2010**, *53*, 3.
22. Barta, T. E.; Veal, J. M.; Rice, J. W.; Partridge, J. M.; Fadden, R. P.; Ma, W.; Jenks, M.; Geng, L.; Hanson, G. J.; Huang, K. H.; Barabasz, A. F.; Foley, B. E.; Otto, J.; Hall, S. E. *Bioorg. Med. Chem. Lett.* **2008**, *18*, 3517.
23. Huang, K. H.; Veal, J. M.; Fadden, R. P.; Rice, J. W.; Eaves, J.; Strachan, J. P.; Barabasz, A. F.; Foley, B. E.; Barta, T. E.; Ma, W.; Silinski, M. A.; Hu, M.; Partridge, J. M.; Scott, A.; DuBois, L. G.; Freed, T.; Steed, P. M.; Ommen, A. J.; Smith, E. D.; Hughes, P. F.; Woodward, A. R.; Hanson, G. J.; McCall, W. S.; Markworth, C. J.; Hinkley, L.; Jenks, M.; Geng, L.; Lewis, M.; Otto, J.; Pronk, B.; Verleysen, K.; Hall, S. E. *J. Med. Chem.* **2009**, *52*, 4288.
24. Gopalsamy, A.; Shi, M.; Golas, J.; Vogan, E.; Jacob, J.; Johnson, M.; Lee, F.; Nilakantan, R.; Petersen, R.; Svenson, K.; Chopra, R.; Tam, M. S.; Wen, Y.; Ellingboe, J.; Arndt, K.; Boschelli, F. *J. Med. Chem.* **2008**, *51*, 373.
25. Driggers, E. M.; Hale, S. P.; Lee, J.; Terrett, N. K. *Nat. Rev. Drug Discov.* **2008**, *7*, 608.
26. Marsault, E.; Peterson, M. L. *J. Med. Chem.* **2011**, *54*, 1961.
27. Zapf, C. W.; Bloom, J. D.; McBean, J. L.; Dushin, R. G.; Nittoli, T.; Ingalls, C.; Southerland, A.; Sonye, J. P.; Eid, C. N.; Golas, J. M.; Liu, H.; Boschelli, F.; Vogan, E. M.; Hu, Y.; Levin, J. I. *Bioorg. Med. Chem. Lett.* **2011**, *21*, 2278.
28. Zapf, C. W.; Bloom, J. D.; McBean, J. L.; Dushin, R. G.; Nittoli, T.; Otteng, M.; Ingalls, C.; Golas, J. M.; Liu, H.; Lucas, J.; Boschelli, F.; Vogan, E. M.; Hu, Y.; Levin, J. I. *Bioorg. Med. Chem. Lett.* **2011**, in press, doi:10.1016/j.bmcl.2011.03.112.
29. Froelich, O.; Desos, P.; Bonin, M.; Quirion, J.-C.; Husson, H.-P.; Zhu, J. *J. Org. Chem.* **1996**, *61*, 6700.
30. The structure has been assigned PDB ID code 3R92.